Biomass Conversion and Biorefinery (2024) 14:19901–19910
https://doi.org/10.1007/s13399-023-03979-3

ORIGINAL ARTICLE

Experimental evaluation of benzene adsorption in the gas phase using activated carbon from waste biomass

Kaan Isinkaralar[1]

Received: 11 January 2023 / Revised: 7 February 2023 / Accepted: 16 February 2023 / Published online: 25 February 2023

Abstract

Benzene is a toxic substance among the volatile organic compounds threatening public health even at low concentrations. Of the many volatiles, it is used in several solvent-based productions and can quickly turn into a gas phase at room temperature. The importance of benzene exposure may be a risk to humans if the amount increases indoors due to an identified carcinogen. However, traditional adsorbents play a lowly role in the purification and separation of benzene. In this paper, the performance of produced adsorbents ($GR_{1\text{-}150}AC$) on benzene removal efficiencies from *Gleditsia riacanthos* L. has been evaluated by chemical activation treatment. Among the tested adsorbents, $GR_{54}AC$ and $GR_{118}AC$ are better than most adsorbents for removing benzene. Here, $GR_{54}AC$ and $GR_{118}AC$ were produced with 1:3 (w/v) H_2SO_4 and 1:4 (w/v) HCl activation at a setting carbonization temperature of 700 and 800 °C, respectively. The pore volumes also reflected the success of HCl and H_2SO_4 activation, which attained $GR_{54}AC$ (894 m^2/g) and $GR_{118}AC$ (748 m^2/g); the total pore volume was 0.43 and 0.24 cm^3/g, while the micropore volume was 0.32 and 0.16 cm^3/g. Moreover, the excellent amount adsorbed with $GR_{54}AC$ varies from 123 to 273 mg/g, and the amount adsorbed of $GR_{118}AC$ increased from 82 to 235 mg/g for 180-min retention time. Results are exciting to assist recent paths for optimizing air filtration systems under actual environmental conditions, particularly regarding its compatibility with the benzene molecular structure of $GR_{54}AC$.

Keywords Environmental exposure · Carbonaceous material · Gas treatment · Green application · VOC removal

1 Introduction

Rapid urbanization, dense residential areas, and industrialization have occasioned critical ambient issues, which are primarily spatial and temporal variations of emerging air pollutants such as benzene [1–3]. It has been a widely used chemical material in products that contributes to decreased air quality [4–6]. Aside from its benzene presence, it also has a proportional relationship with temperature, humidity, and physical and chemical mechanisms. In addition, proximity to outdoor factors (such as gas stations and chemical production facilities) can cause detrimental effects, whereby indoor air is quite effective [7]. Although various sources of benzene are released into the atmosphere, the most crucial mobile source is the storage, refining, transport, and usage of fossil fuels [8–10]. In addition, benzene is found in large amounts in cigarette smoke [11], building materials [12], adhesives [13], solvents [14], cooking [15], and decoration [16]; thus, it can reach high concentrations in indoor air and is even more difficult to control [17].

Benzene negatively affects human health, depending on the degree to which low or high-concentration inhalation would result in confusion, tiredness, leukemia, lymphomas, and death [18, 19]. Besides the damage to humans, benzene is to react with atmospheric hydroxyl free and ozone under air conditions [20]. Therefore, many studies aim to remove and reduce its potential amount for emerging customer requirements by several methods such as incineration [21], condensation [22], biological degradation [23], absorption [24], photo-oxidation [25], membrane separation [26], and adsorption [27]. Among them, the most common and effectively preferred studies have adequately demonstrated that adsorption is a significant process. Benzene removal has emerged by various adsorbents such as biochar [28], metal–organic framework [29], carbon nanotube [30], zeolite [31], organic polymer [32], graphene [33], several

✉ Kaan Isinkaralar
kisinkaralar@kastamonu.edu.tr

[1] Department of Environmental Engineering, Faculty of Engineering and Architecture, Kastamonu University, Kastamonu 37150, Türkiye

composites [34], and activated carbon [35]. Activated carbon is made from different materials; however, lignocellulose-based waste has been increased in the environmentalist understanding [36, 37]. It is preferred because of its process convenience and reasonableness in production, accessibility, applicability, and desorption [38–40]. Especially in recent years, the success of activated carbon obtained by physical or chemical activation to evaluate the waste for the economic cycle [41]. Adsorption methods have been successfully conducted to activate carbons to increase pores' ability and adsorption capacity.

In this work, the preferred species, *Gleditsia riacanthos* L., is widely found in various geographies and is used as folk medicine to treat multiple diseases. The feasibility of activated carbon has been a matter of interest since it sheds its leaves in the winter months. The fallen leaves are disposed of as waste, thus not creating economic value. In this regard, biomass waste has been converted into carbon-based filter material as biosorbents to efficiently remove benzene from the gas atmosphere. Investigating the physicochemical parameters of the produced activated carbons (between GR_1AC and $GR_{150}AC$) and reducing benzene vapor in various concentrations evaluated their efficiency. They are shown to elucidate how efficiency may obtain by capturing benzene molecules. As such, this study aims to offer cautious information for equilibrium data, the adsorption capacity of GRACs, and designing and optimizing the process to availably check out the feasibility of the GRAC filtration about two critical performance criteria (space velocity, particle size, etc.). Overall, it is expected to assist in enlarging the valuable database of GRACs for optimal operation under real-world conditions so it can apply a unique gas filtration system.

2 Materials and methods

2.1 Samples preparation

The leaves of *Gleditsia riacanthos* L. selected carbonaceous material as the precursor for producing GRACs. The precursor was washed with plenty of distilled water to remove the impurities, and then, the drying process was carried out at 48 °C for 2 weeks to remove the moisture. The raw material was sufficiently dried and reduced to a specific size. Afterward, chemical processes were started with 30 g of raw material. It was impregnated with HCl and H_2SO_4 at the ratios of an aqueous solution containing 1:1, 1:2, 1:3, 1:4, and 1:5 (w/v), respectively. Then, the mixture was inserted at 200 °C for 30 min until a paste-like consistency. After, it was kept at room temperature for 24 h and put into the high-temperature resistant reactor for the carbonization process. The mixtures were prepared by being activated at 500, 600, 700, 800, and 900 °C in pure nitrogen gas (N_2) 120 mL/min for 1, 2, and 3 h, respectively. After the reactor was cooled, accompanied by an N_2 atmosphere, samples were taken and washed with hot water until the pH of the filtrate reaches was neutral. Next, they were brought into the oven to dry at 105 °C for 24 h. By weighing, the number of ready samples was labeled as between GR_1AC and $GR_{150}AC$. They were kept in plastic sample bags without contamination until benzene adsorption from the gas phase.

2.2 Structural characterization

The untreated sample (GRB) and post-processed sample (GRACs) were applied as follows: (i) surface functional groups were carried out in the spectrum range of 400–4000 cm^{-1} by Fourier transform infrared spectroscopy (FT-IR, Perkin-Elmer, USA); (ii) porosity was analyzed using a scanning electron microscope (SEM, FEI Quanta FEG 250) as 15 kV and 1000–10,000×; (iii) the Brunauer–Emmett–Teller (BET) was used to measure specific surface area by Quantachrome NOVAtouch LX4 apparatus (South San Francisco, CA, USA); (iv) carbon (C), hydrogen (H), nitrogen (N), and oxygen (O) content were determined by the elemental analyzer (Eurovector, EA3000-Single); (v) the devolatilization behavior of GRB and GRACs was operated under high heating rate conditions between 50 and 850 °C by STA7300 thermal gravimetric analyzer (TGA, HITACHI) following the ASTM D3175-11 [42].

2.3 Batch equilibrium details

GRACs behaviors in Fig. 1 further evaluated the adsorption performance. For this, the differences come to the fore so that the yield comparison can be successful in the equilibrium conditions. Before the GRACs were placed in the reactor, initial benzene concentration was fixed at 3, 6, 9, 13, 16, 26, 42, 54, 70, 86, 102, 128, and 160 mg/m^3 as the gas form. The reactor's inner diameter is 3 cm, and its length is 7 cm, consisting of quartz glass. Experiments were carried out temperature-controlled by determining the benzene evaporator and the initial temperatures of 20, 22, 25, and 30 °C via a thermostat water bath.

Five hundred milligram and 1000 mg of $GR_{54}AC$ and $GR_{118}AC$ were fed into the reactor for adsorption. To better examine the effects of adsorbent amount according to temperature, concentration, and waiting time, the system was operated under control for 2 h until it became stable in 50% relative humidity by a mass flowmeter. After starting the adsorption process with activated carbons, the system was operated intermittently for 3 h. Each measurement is performed using the US EPA Method TO-17 [43]. Tenax tubes were collected for each sample and analyzed TD-GC/MS (Thermal Desorber, Markes Unity)–(Gas chromatography, Thermo Scientific Trace 1300)/(Mass

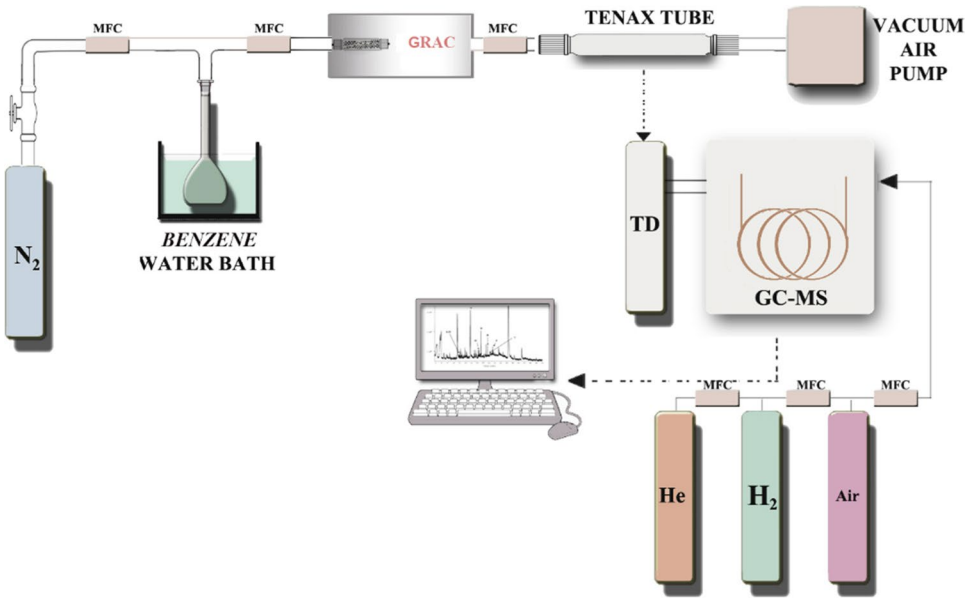

Fig. 1 Schematic diagram of gas adsorption mechanism

detector, Thermo Scientific ISQ QD) and capillary column (TG-624; 30.0 m × 0.25 mm × 1.4 µm) at regular intervals with a flow rate of 20 mL/min N_2 as carrier gas. The saturated benzene adsorption capacity was produced from the breakthrough curve using Eq. (1) reported previous study [44].

$$q_{(mg/g)} = \left(\frac{F\ x\ C_0\ x\ 10^{-9}}{W}\right)\left[\left(\frac{C_i}{C_0}\ x\ t_s\right) - \left(\int_0^{t_s}\frac{C_i}{C_0}d_t\right)\right] \quad (1)$$

where q is the saturated adsorption capacity (mg/g), F is the air speed (mL/min), W is the weight of GRACs (g), C_0 is benzene inflow concentration (mg/m^3), C_i is benzene outflow concentration (mg/m^3), and t_s is saturation time (min).

3 Results and discussion

3.1 Physicochemical properties of GRACs

Benzene adsorption was continued by taking two samples after successful activation processes with the highest surface area and micropore volume. One hundred fifty samples were chemically activated using HCl and H_2SO_4 with particle diameters between 0.22 and 0.54 mm. The increased surface area of $GR_{54}AC$ and $GR_{118}AC$ were obtained with 1:4 (w/v) HCl at 800 °C and 1:3 (w/v) H_2SO_4 at 700 °C. The carbon ratio of GRB was 45.24%, while the highest was 66.92% in $GR_{118}AC$ and 71.91% in $GR_{54}AC$. Volatile substances were determined as 69.06% in GRB, and after carbonization, $GR_{54}AC$ and $GR_{118}AC$, 19.82% and 23.65%, respectively. Also, the amounts of H, O, N, moisture, and ash significantly decrease; however, the fixed carbon amount remarkably increases in Table 1.

Figure 2 shows SEM images of samples in the large porosity and structure destroyed by the activating agents. There were many remarkable differences in the surface morphology and roughness of raw samples compared to the GRACs. Previous studies reported that the corrosive effect of chemicals on pore structure could be similar to this study [45]. The development in the structure morphology has been revealed, which can be considered almost at the medium level. It has been observed that the design variations result from different activation chemicals used in each of them.

FT-IR spectra of the GRB, $GR_{54}AC$, and $GR_{118}AC$ are displayed in Fig. 3. It is identified which changes functional groups (carboxyl, carboxylic anhydride, phenol, lactone, etc.) on their surface from acid or base via absorption peaks. Carbon metrix occurs by heteroatoms such as H_2, N_2, and O_2, forming the surface chemistry of GRACs [46]. The significant peaks at 3589 cm^{-1} represent the stretching

Table 1 Elemental and chemical components (wt%) of GRACs

Analysis type	Content	Selected materials		
		GRB	$GR_{54}AC$	$GR_{118}AC$
Elemental	C	45.24	71.91	66.92
	H	5.67	2.84	2.36
	O	46.22	24.43	16.84
	N	2.87	0.82	0.66
Chemical	Moisture	5.37	2.35	3.16
	Volatile substant	69.06	19.82	23.65
	Fixed carbon	22.86	76.56	70.02
	Ash	2.71	1.27	3.17

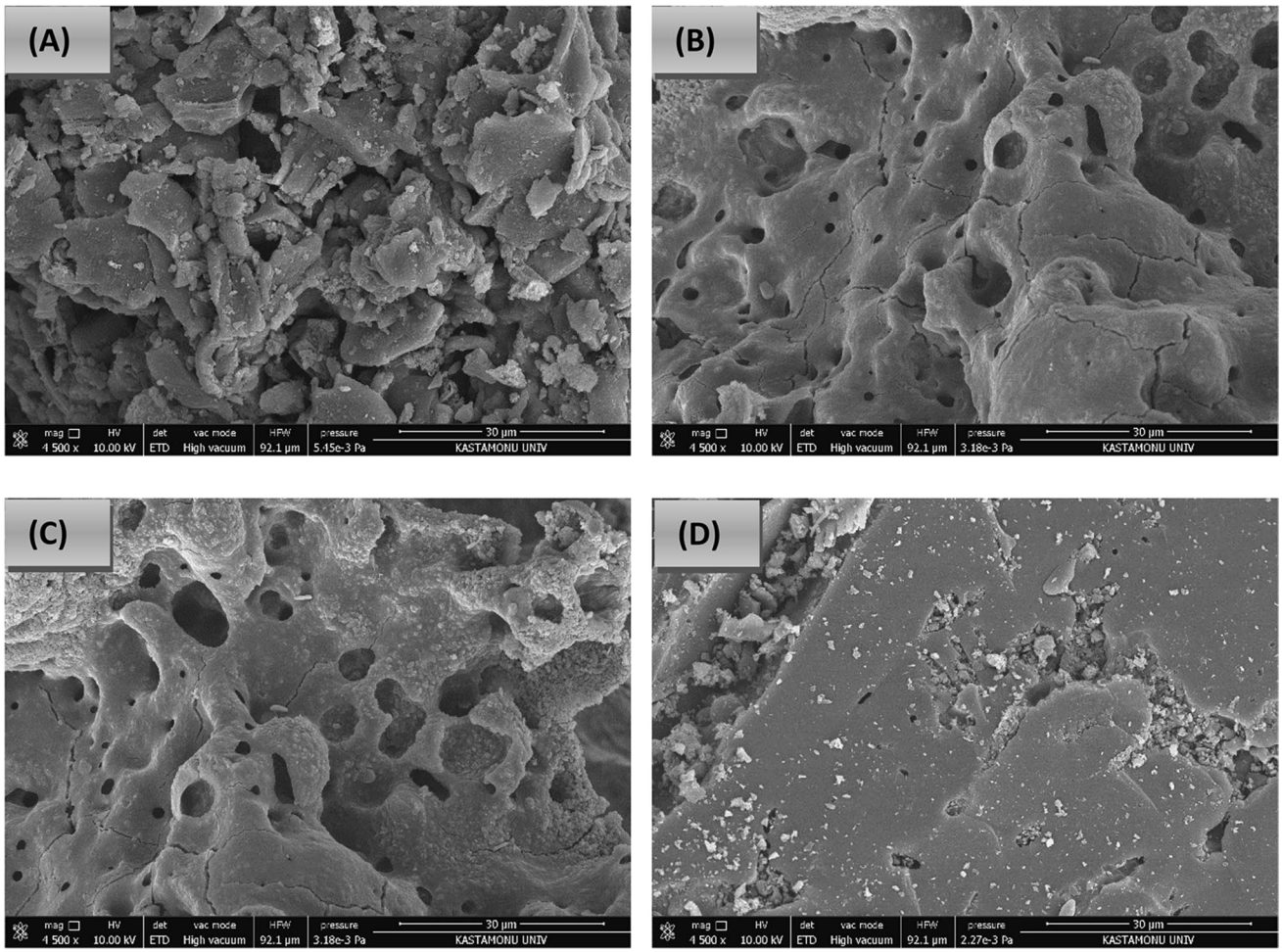

Fig. 2 SEM micrographs of GRB (**A**), $GR_{54}AC$ (**B**), $GR_{118}AC$ (**C**), and after adsorption $GR_{54}AC$ (**D**)

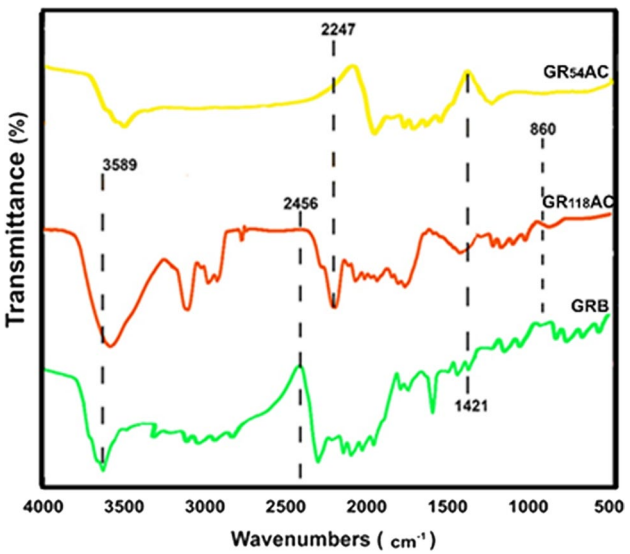

Fig. 3 FT-IR spectra of GRB, $GR_{54}AC$, and $GR_{118}AC$

vibration of the O–H bond of carboxyl and phenol [47, 48]. The region where the weak peaks observed between 2900 and 3100 cm^{-1} could be dedicated to the stretching vibration of –OH, $–CH_2–$, or carboxyl carbonates structures and the stretching vibration O–H group during the activation processes, respectively. The prominent peak comprises 1678 cm^{-1} appointed to the C = O in stretching vibration in aliphatic ketone and aromatic rings [49, 50]. The other firm peaks at 985 cm^{-1}, providing a reaction between amino groups and chloride compounds. The band at 860 cm^{-1} is associated with the out-of-plane bending vibration of O–H. Also, values less than 800 cm^{-1} correspond to the stretching vibration of the (C-S)-others bond [51].

3.1.1 TGA

According to Fig. 4, the TGA thermograms of the GRB, $GR_{54}AC$, and $GR_{118}AC$ were analyzed in the weight loss curves, which show three primary decompositions at 70 °C, 358–470 °C, and 610–726 °C that can describe loss

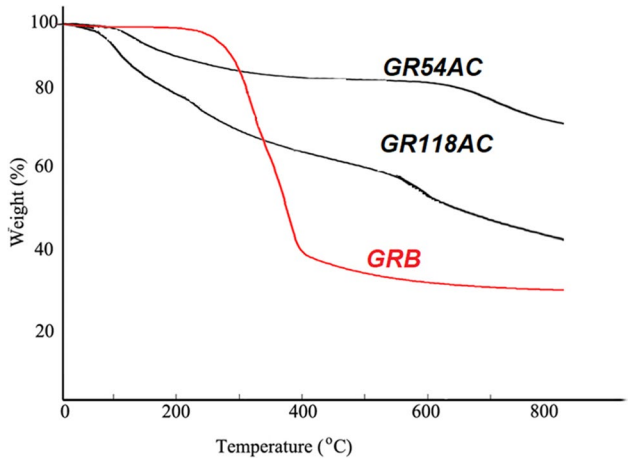

Fig. 4 Thermal treatment curves of GRB, $GR_{54}AC$, and $GR_{118}AC$

Table 2 Pore structure parameters of GRB, $GR_{54}AC$, and $GR_{118}AC$

Materials	GRB	$GR_{54}AC$	$GR_{118}AC$
S_{BET} (m^2/g)	7	894	748
V_{total} (cm^3/g)	0.02	0.43	0.24
V_{micro} (cm^3/g)	-	0.32	0.16
V_{meso} (cm^3/g)	-	0.11	0.08
Dp (nm)	-	1.88	1.68

(around 11–28%) of H_2O, CO_2, and CO, respectively [52]. A systematic decrease and rate loss were observed in all weight samples due to the different volatility of compounds. Until 250 °C, weight loss pertains to interlayer water and surface adsorption evaporation; however, 400–800 °C is essential for GRACs combustion [53]. There is no remarkable difference between $GR_{54}AC$ and $GR_{118}AC$ because chemical activation did not affect the main surface.

The specific surface area (S_{BET}), micropore volume (V_{micro}), mesopore volume (V_{meso}), total pore volume (V_{total}) at $P/P_0 = 0.99$, and average pore diameter (Dp) of the samples are given in Table 2. As can be seen, it was stated that the surface area increased from 7 to 748 m^2/g and 894 m^2/g via chemical activation. Total pore volume was reflected at 0.43 cm^3/g and 0.24 cm^3/g in $GR_{54}AC$ and $GR_{118}AC$, while micropore volume was 0.32 cm^3/g and 0.16 cm^3/g.

3.2 Adsorbing capacity

3.2.1 Initial concentration

In order to determine the stable conditions of the system as the optimum conditions of the setup set up in the laboratory, a total of 13 different benzene concentrations were selected, with initial concentrations ranging from 3 to 160 mg/m^3. A batch reactor also can control temperature, and the movement-adhesion of benzene molecules was investigated by changing the ambient temperatures. $GR_{54}AC$ and $GR_{118}AC$ studied the adsorption capacities of the determined concentrations in the reactor at atmospheric pressure and 20, 22, 25, and 30 °C. In general, the ability of both adsorbents at low concentrations was considerably lower than at high concentrations. However, as the concentration increased, there were differences in the increase according to the physicochemical properties of the adsorbent. The amount adsorbed with 0.5 g of $GR_{54}AC$ was 123, 131, 148, and 202 mg/g at 20, 22, 25, and 30 °C, respectively. The amount adsorbed with 1 g of $GR_{54}AC$ was 181, 226, 273, and 256 mg/g. The amount adsorbed with 0.5 g of $GR_{118}AC$ was 82, 104, 117, and 131 mg/g at 20, 22, 25, and 30 °C, respectively; the amount adsorbed with 1 g of $GR_{118}AC$ was 148, 201, 235, and 226 mg/g, respectively. The movement and behavior of benzene molecules at 20 °C differed markedly from those at 30 °C. The main reason for this is thought to be the increase in the boiling point of benzene molecules. In addition, it is believed that the benzene molecule settles in the adsorbents, which occurs with the decrease of the moisture content in Fig. 5.

3.2.2 Residence time

It is seen that the residence time is parallel to the increase in the rate of penetration of benzene molecules into the adsorbent and settling there. As the time increased, it was determined that the pores were filled, but the temperature factor prolonged the adsorption time. The increased temperature affected from 20 to 30 °C in experiments using $GR_{54}AC$ and $GR_{118}AC$ in Fig. 6.

Various methods have been developed to remove benzene from the gas environment and reduce the risk to human health due to its adverse effects. However, the transfer and bonding of benzene molecules in the adsorbents have not been investigated yet, as far as the present investigators know, and it remains to be answered to abate the harmful gas-phase benzene under several conditions. Among techniques, adsorption has become an effective process for removing benzene by biosorbents owing to its characteristics of cost-effectiveness [54–56]. Among the adsorbents used in gas-phase benzene filtration, environmentally friendly, and low-budget activated carbons were used from various raw materials [57–59]. Biomass denotes biological materials from plant sources (including agricultural, forestry, and woody plants) and their derived residue and waste as a sustainable resource by woody plants utilizing thermochemical, biochemical, and physicochemical technology [60, 61]. In all cases, the removal of benzene with different conditions has been studied with the developed filter materials and adsorbents that lignocellulosic biomass

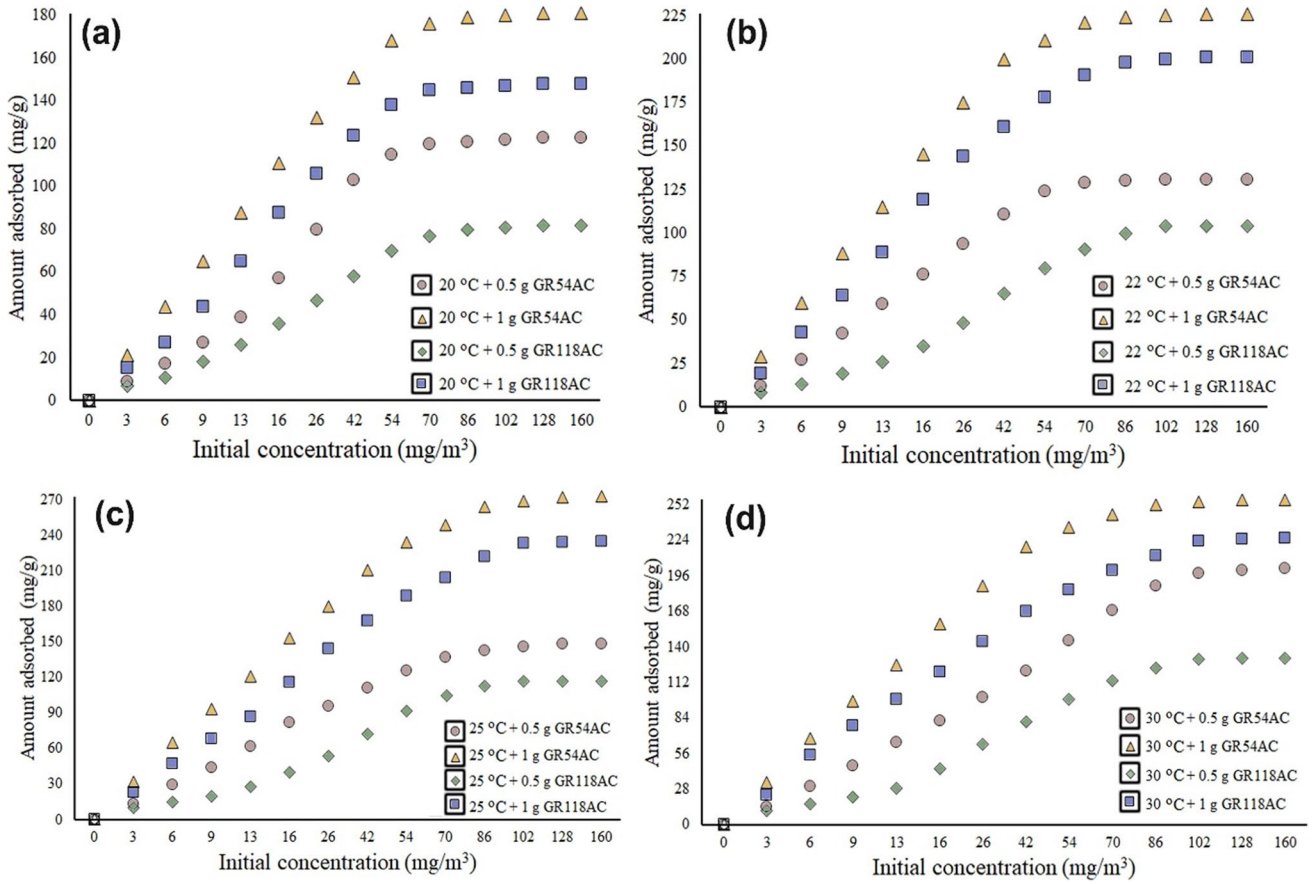

Fig. 5 Effect of initial concentration of the adsorbed amount

is over-pioneering thanks to their accessibility properties [62, 63].

Here, differences such as ambient parameters, temperature, humidity, initial conditions, amount of adsorbent used, and intermittent, sequential, or continuous flow bed reactor have emerged to reduce benzene molecules on the adsorbents for widespread gas applications. Generally, there is a considerable number of benzene removal studies at the laboratory scale; however, there is also a lack of research on real environments. The adsorption capacity is affected by humidity which can sharply fill the pores because water molecules will replace part of the adsorbed benzene. Ha et al. [64] evaluated gas-benzene adsorption using 200 mg of commercial activated carbon in a filter bed system. The adsorption capacity for 10 ppm initial benzene concentration was compared between PAC and GAC at different flow rates, and they applied three kinetic models to assess benzene adsorption. Karimnezhad et al. [65] prepared activated carbons derived from the walnut shell via $ZnCl_2$ chemical activation and found a surface area of 2643 m^2/g. They investigated benzene removal with 0.11 g synthesized activated carbon, and benzene capacity reached 180 to 510 mg at 1100 ppm. Stähelin et al. [66] used an adsorbent obtained from a coconut shell, and it assessed benzene and toluene adsorption range from 10 to 200 g/L as a solvent in a bicomponent adsorption mechanism. This work aimed to reduce their concentration when compared to the monocomponent apparatus. By comparing the results, it was deduced that a slow rate had in the benzene monocomponent system. Still, the holding capacity had a higher value with monolayer adsorption than in other systems.

Maitlo et al. [67] demonstrated that toluene and ethyl benzene, as other VOCs, were performed to the effect of contact time, adsorbent amount, etc., in a batch reactor. They found adsorbed amount differences in molecular behavior due to toluene being more soluble than ethylbenzene. Among those mentioned above, the predominant mechanisms of volatile compound capture would vary by environmental conditions. Generally, molecules are occupied with physical adsorption on sites to the findings of Abedi et al. [68]. This finding also implied that the various adsorbent shows enhanced physicochemical interactions on their surface. Based on the types of adsorbents assisted in highly increased diffusivity of benzene performance, however, the adsorption rate of benzene was reduced under various operation conditions. The adsorption of gaseous benzene was investigated and

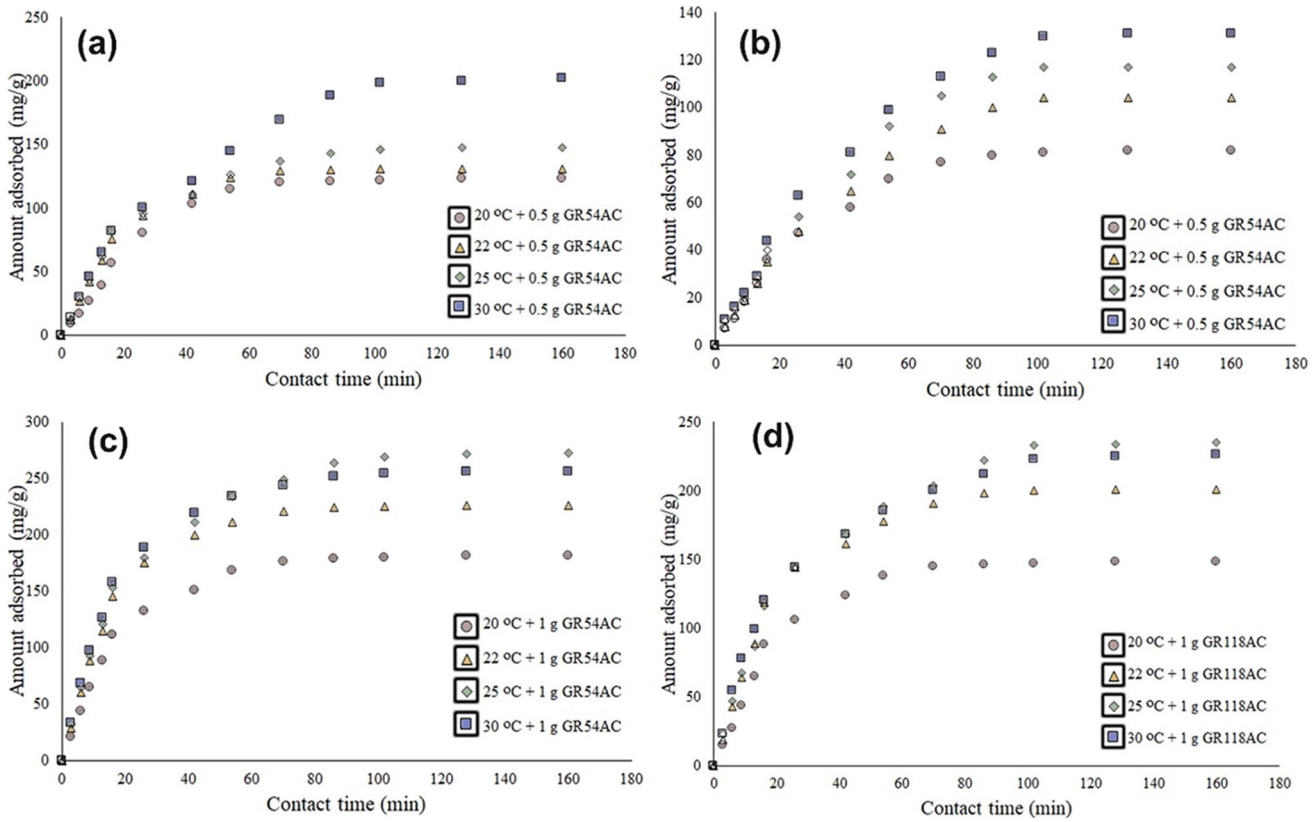

Fig. 6 Effect of contact time of adsorbed amount

analyzed in the research of Khan et al. [69]. They used to observe sorption performance onto several adsorbents such as zeolite, activated carbon, tea leaves, ground coffee, and Carbopack-X for 50-ppm inlet value at room temperature by gas chromatography with flame ionization detector (GC-FID). The adsorption behavior was investigated for all sorbents, and the maximum adsorption capacity was found to be 79.1 mg/g for ACd212. The gaseous benzene adsorption mechanisms were tried to understand their behavior on composite materials. The summary of the study contributes to recovery or destruction experiments based on whether the benzene can be recovered. As mentioned before, the interactions between benzene and $GR_{54}AC$ have been intensively discussed for modification to enhance adsorption performance. In the research of Ma et al. [70], they investigated selected VOCs (benzene, toluene, o-xylene, p-xylene, and chlorobenzene) adsorption capacity on commercial activated carbon, which surface area and total pore volume are 996. 32 m^2/g and 0.4861 cm^3/g from flue gas in a fixed-bed reactor. Three VOCs were studied using a gas adsorption analyzer at 120 °C and calculated by the breakthrough curve. In their benzene experiments, outlet concentration remained stable at 115 min; however, benzene molecules almost sold out at 20 min. Low VOC adsorption capacities were mainly found from 12.3 to 52.7 mg/g, and physical adsorption was suitable under certain conditions. Significantly influences the improvement of better benzene removal performance on other adsorbents relative to others.

Anand et al. [71] investigated the effects of metal–organic frameworks (MOFs) called Co-CUK-1. It exhibited adsorptive removal of gaseous benzene (0.5, 1, 5, and 10 ppm) at 298 K. Porous MOFs of metal ions with a high usable charge density were bound more strongly to benzene molecules and associated with adsorption capacity. Osuchowski et al. [72] synthesized the carbon spheres (S_{BET}: 990 m^2/g and total pore volume (V_t) of 1.32 cm^3/g), preparing analogous synthetic procedure and benzene vapor adsorption investigated on the selected sorbents. The maximum capacity effect could be more significant if highly porous carbons are closely contacted. Hassan and Sorial [73] introduced an experiment design: trickle bed air biofilter (TBAB) removal of benzene at 25 °C and initially at an influent concentration of 355 ppmv. The TBAB was obtained to successful performance and capacity with 90% and 58 $g/(m^3h)$. At the same time, there is no noticeable difference in non-polar aromatic VOC removal performance that can be decreased significantly under several treatments and sorbents. For the applications of $GR_{54}AC$ on benzene removal, it is clear that the $GR_{54}AC$ can dominate the VOCs adsorption application market, and very few practices adopt other adsorbents. Due

to its low cost, high chemical stability, and non-toxic properties, $GR_{54}AC$ has largely been enquired about and applied to the favorable applications on benzene adsorption. Since lignocellulosic wastes have different properties, other waste biomass will also be applied to other VOCs soon according to their specific properties.

4 Conclusion

In this study, the capture yields of $GR_{54}AC$ and $GR_{118}AC$ were investigated in different temperatures, concentrations, adsorbent amounts, and time-dependent conditions. The $GR_{54}AC$ is the most efficient and high-performance approach to preventing benzene. It is positively differentiated from the others with its physicochemical properties and capturing conditions. The main reason for the difference in adsorption was caused by micropore volume, pore structure, and the ambient temperature factor in the acceleration of the benzene molecules. Additionally, the adsorption efficiency at high benzene concentrations onto $GR_{54}AC$ gave better results than the low concentration. The main reason is the different rates of filling the pores of dense particles. In the extended period to reach equilibrium conditions, the situation seen is that the adhesion rate of the adsorbents decreases, even almost non-existent. It has been determined that the increase in the amount used, the variability in the equilibrium conditions, the increase in adhesion amount, flow rates, and the transport of benzene molecules have been determined to play a dominant role in the adsorption mechanism. The results were obtained by comparing the advection benzene molecular through the $GR_{54}AC$ and the $GR_{118}AC$. It is promising for future studies that the usability of $GR_{54}AC$ filter systems will be investigated in how $GR_{54}AC$ removal efficiency compare and assessed in sustainable green technology.

Author contribution This study is written entirely by Kaan Isinkaralar.

Data availability The data that support the findings of this study are available from the corresponding author, upon reasonable request.

Declarations

Ethics approval Not applicable.

Competing interest The author declares no competing interests.

References

1. Linden J, Boman J, Holmer B, Thorsson S, Eliasson I (2012) Intra-urban air pollution in a rapidly growing Sahelian city. Environ Int 40:51–62. https://doi.org/10.1016/j.envint.2011.11.005
2. Isinkaralar O, Varol C, Yilmaz D (2022) Digital mapping and predicting the urban growth: integrating scenarios into cellular automata—Markov chain modeling. Appl Geomat 14(4):695–705. https://doi.org/10.1007/s12518-022-00464-w
3. Isinkaralar O, Varol C (2023) A cellular automata-based approach for spatio-temporal modeling of the city center as a complex system: the case of Kastamonu, Türkiye. Cities 132:104073. https://doi.org/10.1016/j.cities.2022.104073
4. Ong CN, Lee BL (1994) Determination of benzene and its metabolites: application in biological monitoring of environmental and occupational exposure to benzene. J Chromatogr B Biomed Sci Appl 660(1):1–22. https://doi.org/10.1016/0378-4347(94)00278-9
5. Gentry JC (2007) Benzene production and economics: a review. Asia-Pac J Chem Eng 2(4):272–277. https://doi.org/10.1002/apj.18
6. Miller D, Armstrong K, Styring P (2022) Assessing methods for the production of renewable benzene. Sustain Prod Consum 32:184–197. https://doi.org/10.1016/j.spc.2022.04.019
7. Sinha SN, Kulkarni PK, Shah SH, Desai NM, Patel GM, Mansuri MM, Saiyed HN (2006) Environmental monitoring of benzene and toluene produced in indoor air due to combustion of solid biomass fuels. Sci Total Environ 357(1–3):280–287. https://doi.org/10.1016/j.scitotenv.2005.08.011
8. Roberts DW (2003) Optimisation of the linear alkyl benzene sulfonation process for surfactant manufacture. Org Process Res Dev 7(2):172–184. https://doi.org/10.1021/op020088w
9. Ji Y, Gao F, Wu Z, Li L, Li D, Zhang H, Zhang Y, Gao J, Bai Y, Li H (2020) A review of atmospheric benzene homologues in China: characterization, health risk assessment, source identification and countermeasures. J Environ Sci 95:225–239. https://doi.org/10.1016/j.jes.2020.03.035
10. Zhang R, Zeng L, Wang F, Li X, Li Z (2022) Influence of pore volume and surface area on benzene adsorption capacity of activated carbons in indoor environments. Build Environ 216:109011. https://doi.org/10.1016/j.buildenv.2022.109011
11. Kaunelienė V, Meišutovič-Akhtarieva M, Martuzevičius D (2018) A review of the impacts of tobacco heating system on indoor air quality versus conventional pollution sources. Chemosphere 206:568–578. https://doi.org/10.1016/j.chemosphere.2018.05.039
12. Brdarić D, Kovač-Andrić E, Šapina M, Kramarić K, Lutz N, Perković T, Egorov A (2019) Indoor air pollution with benzene, formaldehyde, and nitrogen dioxide in schools in Osijek, Croatia. Air Qual Atmos Health 12:963–968. https://doi.org/10.1007/s11869-019-00715-7
13. Zhao Z, Pei Y, Zhao P, Wu C, Qu C, Li W, Zhao Y, Liu J (2022) Characterizing key volatile pollutants emitted from adhesives by chemical compositions, odor contributions and health risks. Molecules 27(3):1125. https://doi.org/10.3390/molecules27031125
14. Cui X, Ma J, Li H (2022) The effect of diluent on the release of benzene series from nitrocellulose-lacquered MDF. Atmosphere 14(1):21. https://doi.org/10.3390/atmos14010021
15. Li W, Wang H, Li C, Yu CW (2021) Control of temperature and fume generation by cooking in a residential kitchen by ceiling radiative cooling and fume hood extraction. Indoor Built Environ 30(8):1211–1225. https://doi.org/10.1177/1420326X20945750
16. Song G, Yu A, Sakai K, Khalequzzaman M, Nakajima T, Kitamura F, Guo P, Yokoyama K, Piao F (2017) Levels of volatile organic compounds in homes in Dalian, China. Air Qual Atmos Health 10:171–181. https://doi.org/10.1007/s11869-016-0422-3
17. Mukherjee B, Dutta A, Roychoudhury S, Ray MR (2013) Chronic inhalation of biomass smoke is associated with DNA damage in airway cells: involvement of particulate pollutants and benzene. J Appl Toxicol 33(4):281–289. https://doi.org/10.1002/jat.1748

18. Schnatter AR, Rosamilia K, Wojcik NC (2005) Review of the literature on benzene exposure and leukemia subtypes. Chem Biol Interact 153:9–21. https://doi.org/10.1016/j.cbi.2005.03.039
19. Bulka C, Nastoupil LJ, McClellan W, Ambinder A, Phillips A, Ward K, Bayakly AR, Switchenko JM, Waller L, Flowers CR (2013) Residence proximity to benzene release sites is associated with increased incidence of non-Hodgkin lymphoma. Cancer 119(18):3309–3317
20. Einaga H, Teraoka Y, Ogata A (2013) Catalytic oxidation of benzene by ozone over manganese oxides supported on USY zeolite. J Catal 305:227–237. https://doi.org/10.1016/j.jcat.2013.05.016
21. Lei Y, Zhao G, Zhang Y, Liu M, Liu L, Lv B, Gao J (2010) Highly efficient and mild electrochemical incineration: mechanism and kinetic process of refractory aromatic hydrocarbon pollutants on superhydrophobic PbO2 anode. Environ Sci Technol 44(20):7921–7927. https://doi.org/10.1021/es101693h
22. Kinder KM, Gellasch CA, Dusenbury JS, Timmes TC, Hughes TM (2017) Evaluating the impact of ambient benzene vapor concentrations on product water from Condensation Water From Air technology. Sci Total Environ 590:60–68. https://doi.org/10.1016/j.scitotenv.2017.02.171
23. Yoshikawa M, Zhang M, Toyota K (2017) Integrated anaerobic-aerobic biodegradation of multiple contaminants including chlorinated ethylenes, benzene, toluene, and dichloromethane. Water Air Soil Pollut 228:1–13. https://doi.org/10.1007/s11270-016-3216-1
24. Läntelä J, Rasi S, Lehtinen J, Rintala J (2012) Landfill gas upgrading with pilot-scale water scrubber: performance assessment with absorption water recycling. Appl Energy 92:307–314. https://doi.org/10.1016/j.apenergy.2011.10.011
25. Borrás E, Tortajada-Genaro LA (2012) Secondary organic aerosol formation from the photo-oxidation of benzene. Atmos Environ 47:154–163. https://doi.org/10.1016/j.atmosenv.2011.11.020
26. Dalane K, Dai Z, Mogseth G, Hillestad M, Deng L (2017) Potential applications of membrane separation for subsea natural gas processing: a review. Journal of Natural Gas Science and Engineering 39:101–117. https://doi.org/10.1016/j.jngse.2017.01.023
27. Zhu L, Shen D, Luo KH (2020) A critical review on VOCs adsorption by different porous materials: species, mechanisms and modification methods. J Hazard Mater 389:122102. https://doi.org/10.1016/j.jhazmat.2020.122102
28. Buss W, Mašek O (2016) High-VOC biochar—effectiveness of post-treatment measures and potential health risks related to handling and storage. Environ Sci Pollut Res 23:19580–19589. https://doi.org/10.1007/s11356-016-7112-4
29. Bhattarai DP, Pant B, Acharya J, Park M, Ojha GP (2021) Recent progress in metal–organic framework-derived nanostructures in the removal of volatile organic compounds. Molecules 26(16):4948. https://doi.org/10.3390/molecules26164948
30. Yoosefian M, Ayoubi E, Atanase LI (2022) Palladium-doped single-walled carbon nanotubes as a new adsorbent for detecting and trapping volatile organic compounds: a first principle study. Nanomaterials 12(15):2572. https://doi.org/10.3390/nano12152572
31. Derakhshan-Nejad A, Rangkooy HA, Cheraghi M, Yengejeh RJ (2020) Removal of ethyl benzene vapor pollutant from the air using TiO 2 nanoparticles immobilized on the ZSM-5 zeolite under UVradiation in lab scale. J Environ Health Sci Eng 18:201–209. https://doi.org/10.1007/s40201-020-00453-4
32. Chabbah T, Abderrazak H, Saint Martin P, Casabianca H, Kricheldorf HR, Chatti S (2020) Synthesis of Glux based polymers for removal of benzene derivatives and pesticides from water. Polym Adv Technol 31(10):2339–2350. https://doi.org/10.1002/pat.4953
33. Rahbar Shamskar K, Rashidi A, Aberoomand Azar P, Yousefi M, Baniyaghoob S (2019) Synthesis of graphene by in situ catalytic chemical vapor deposition of reed as a carbon source for VOC adsorption. Environ Sci Pollut Res 26:3643–3650. https://doi.org/10.1007/s11356-018-3799-8
34. Palmieri S, Pierpaoli M, Riderelli L, Qi S, Ruello ML (2020) Preparation and characterization of an electrospun PLA-cyclodextrins composite for simultaneous high-efficiency PM and VOC removal. Journal of Composites Science 4(2):79. https://doi.org/10.3390/jcs4020079
35. Isinkaralar K (2022) High-efficiency removal of benzene vapor using activated carbon from Althaea officinalis L. biomass as a lignocellulosic precursor. Environ Sci Pollut Res 29(44):66728–66740. https://doi.org/10.1007/s11356-022-20579-2
36. Zaitan H, Korrir A, Chafik T, Bianchi D (2013) Evaluation of the potential of volatile organic compound (di-methyl benzene) removal using adsorption on natural minerals compared to commercial oxides. J Hazard Mater 262:365–376. https://doi.org/10.1016/j.jhazmat.2013.08.071
37. Tang W, Wu X, Li S, Shan X, Liu G, Chen Y (2015) Co-nanocasting synthesis of mesoporous Cu–Mn composite oxides and their promoted catalytic activities for gaseous benzene removal. Appl Catal B 162:110–121. https://doi.org/10.1016/j.apcatb.2014.06.030
38. Wibowo N, Setyadhi L, Wibowo D, Setiawan J, Ismadji S (2007) Adsorption of benzene and toluene from aqueous solutions onto activated carbon and its acid and heat treated forms: influence of surface chemistry on adsorption. J Hazard Mater 146(1–2):237–242. https://doi.org/10.1016/j.jhazmat.2006.12.011
39. Veksha A, Sasaoka E, Uddin MA (2009) The influence of porosity and surface oxygen groups of peat-based activated carbons on benzene adsorption from dry and humid air. Carbon 47(10):2371–2378. https://doi.org/10.1016/j.carbon.2009.04.028
40. Isinkaralar K, Turkyilmaz A (2022) Simultaneous adsorption of selected VOCs in the gas environment by low-cost adsorbent from Ricinus communis. Carbon Letters 32(7):1781–1789. https://doi.org/10.1007/s42823-022-00399-7
41. Isinkaralar K (2022) Theoretical removal study of gas BTEX onto activated carbon produced from Digitalis purpurea L biomass. Biomass Convers Biorefin 12(9):4171–4181. https://doi.org/10.1007/s13399-022-02558-2
42. ASTM (2011) Standard test method for volatile matter in the analysis sample of coal and coke. D3175–11
43. US EPA (1999) Determination of volatile organic compounds in ambient air using active sampling onto sorbent tubes, compendium of methods for the determination of toxic organic compounds in ambient air, Second Edition Compendium Method TO-17, U.S. Environmental Protection Agency (US EPA), Washington, DC.
44. Lv Y, Sun J, Yu G, Wang W, Song Z, Zhao X, Mao Y (2020) Hydrophobic design of adsorbent for VOC removal in humid environment and quick regeneration by microwave. Microporous Mesoporous Mat 294:109869. https://doi.org/10.1016/j.micromeso.2019.109869
45. Kang S, Baginska M, White SR, Sottos NR (2015) Core–shell polymeric microcapsules with superior thermal and solvent stability. ACS Appl Mater Interfaces 7(20):10952–10956. https://doi.org/10.1021/acsami.5b02169
46. Kumar A, Jena HM (2016) Preparation and characterization of high surface area activated carbon from Fox nut (Euryale ferox) shell by chemical activation with H3PO4. Results Phys 6:651–658. https://doi.org/10.1016/j.rinp.2016.09.012
47. González-García P, Centeno TA, Urones-Garrote E, Ávila-Brande D, Otero-Díaz LC (2013) Microstructure and surface properties of lignocellulosic-based activated carbons. Appl Surf Sci 265:731–737. https://doi.org/10.1016/j.apsusc.2012.11.092
48. Pezoti O, Cazetta AL, Bedin KC, Souza LS, Martins AC, Silva TL, Junior OOS, Visentainer JV, Almeida VC (2016) NaOH-activated carbon of high surface area produced from guava seeds

as a high-efficiency adsorbent for amoxicillin removal: Kinetic, isotherm and thermodynamic studies. Chem Eng J 288:778–788. https://doi.org/10.1016/j.cej.2015.12.042
49. Cao W, Cao C, Guo L, Jin H, Dargusch M, Bernhardt D, Yao X (2016) Hydrogen production from supercritical water gasification of chicken manure. Int J Hydrogen Energy 41(48):22722–22731. https://doi.org/10.1016/j.ijhydene.2016.09.031
50. Mistar EM, Alfatah T, Supardan MD (2020) Synthesis and characterization of activated carbon from Bambusa vulgaris striata using two-step KOH activation. J Market Res 9(3):6278–6286. https://doi.org/10.1016/j.jmrt.2020.03.041
51. Najafi A, Golestani-Fard F, Rezaie HR, Ehsani N (2011) A study on sol–gel synthesis and characterization of SiC nano powder. J Sol-Gel Sci Technol 59(2):205–214. https://doi.org/10.1007/s10971-011-2482-z
52. Jakab E, Omastová M (2005) Thermal decomposition of polyolefin/carbon black composites. J Anal Appl Pyrol 74(1–2):204–214. https://doi.org/10.1016/j.jaap.2005.02.001
53. Liu YH, Hsi HC, Li KC, Hou CH (2016) Electrodeposited manganese dioxide/activated carbon composite as a high-performance electrode material for capacitive deionization. ACS Sustain Chem Eng 4(9):4762–4770. https://doi.org/10.1021/acssuschemeng.6b00974
54. Chavadej S, Kiatubolpaiboon W, Rangsunvigit P, Sreethawong T (2007) A combined multistage corona discharge and catalytic system for gaseous benzene removal. J Mol Catal A: Chem 263(1–2):128–136. https://doi.org/10.1016/j.molcata.2006.08.061
55. Takeuchi M, Hidaka M, Anpo M (2012) Efficient removal of toluene and benzene in gas phase by the TiO2/Y-zeolite hybrid photocatalyst. J Hazard Mater 237:133–139. https://doi.org/10.1016/j.jhazmat.2012.08.011
56. Saleem F, Khoja AH, Umer J, Ahmad F, Abbas SZ, Zhang K, Harvey A (2021) Removal of benzene as a tar model compound from a gas mixture using non-thermal plasma dielectric barrier discharge reactor. J Energy Inst 96:97–105. https://doi.org/10.1016/j.joei.2021.02.008
57. Vohra MS (2015) Adsorption-based removal of gas-phase benzene using granular activated carbon (GAC) produced from date palm pits. Arab J Sci Eng 40(11):3007–3017. https://doi.org/10.1007/s13369-015-1683-0
58. Deng Z, Deng Q, Wang L, Xiang P, Lin J, Murugadoss V, Song G (2021) Modifying coconut shell activated carbon for improved purification of benzene from volatile organic waste gas. Advanced Composites and Hybrid Materials 4(3):751–760. https://doi.org/10.1007/s42114-021-00273-6
59. Jeong M, Zhao S, Ji Y, Khan SA, Saqlain S, Kim YD (2022) Efficacious removal of benzene and ammonia gases over visible light irradiated activated carbon. Appl Surf Sci 156012. https://doi.org/10.1016/j.apsusc.2022.156012
60. Szulejko JE, Kim KH, Parise J (2019) Seeking the most powerful and practical real-world sorbents for gaseous benzene as a representative volatile organic compound based on performance metrics. Sep Purif Technol 212:980–985. https://doi.org/10.1016/j.seppur.2018.11.001
61. Rashidi R, Moussavi G, Khavanin A, Ghaderpoori A (2019) The efficacy of the ozonation process in the presence of activated carbon impregnated with magnesium oxide in the removal of benzene from the air stream. Int J Environ Sci Technol 16(12):8023–8030. https://doi.org/10.1007/s13762-019-02239-0
62. de Mello R, Motheo AJ, Saez C, Rodrigo MA (2022) Combination of granular activated carbon adsorption and electrochemical oxidation processes in methanol medium for benzene removal. Electrochimica Acta, 140681. https://doi.org/10.1016/j.electacta.2022.140681
63. Alshahrani F, Tawabini B, Saleh T, Alrayaan M, Alaama S, Nasser R, Soupious P, Kirmizakis P, Mahmoud M, Oyehan T, Safi E (2022) Removal of benzene, MTBE and toluene from contaminated waters using biochar-based liquid activated carbon. Sci Rep 12(1):1–11. https://doi.org/10.1038/s41598-022-24283-6
64. Ha SH, Kim KH, Younis SA, Dou X (2020) The interactive roles of space velocity and particle size in a microporous carbon bed system in controlling adsorptive removal of gaseous benzene under ambient conditions. Chem Eng J 401:126010. https://doi.org/10.1016/j.cej.2020.126010
65. Karimnezhad L, Haghighi M, Fatehifar E (2014) Adsorption of benzene and toluene from waste gas using activated carbon activated by $ZnCl_2$. Front Environ Sci Eng 8(6):835–844. https://doi.org/10.1007/s11783-014-0695-4
66. Stähelin PM, Valério A, Ulson SMDAG, da Silva A, Valle JAB, de Souza AAU (2018) Benzene and toluene removal from synthetic automotive gasoline by mono and bicomponent adsorption process. Fuel 231:45–52. https://doi.org/10.1016/j.fuel.2018.04.169
67. Maitlo HA, Maitlo G, Song X, Zhou M, Kim KH (2022) A figure of merits-based performance comparison of various advanced functional nanomaterials for adsorptive removal of gaseous ammonia. Sci Total Environ 153428. https://doi.org/10.1016/j.scitotenv.2022.153428
68. Abedi Z, Assadi A, Farahmandkia Z, Mehrasebi MR (2019) The effect of natural organic compounds on the adsorption of toluene and ethylene benzene on MWCNT. J Environ Health Sci Eng 17:1055–1065. https://doi.org/10.1007/s40201-019-00420-8
69. Khan A, Szulejko JE, Kim KH, Sammadar P, Lee SS, Yang X, Ok YS (2019) A comparison of figure of merit (FOM) for various materials in adsorptive removal of benzene under ambient temperature and pressure. Environ Res 168:96–108. https://doi.org/10.1016/j.envres.2018.09.019
70. Ma X, Yang L, Wu H (2021) Removal of volatile organic compounds from the coal-fired flue gas by adsorption on activated carbon. J Clean Prod 302:126925. https://doi.org/10.1016/j.jclepro.2021.126925
71. Anand B, Szulejko JE, Kim KH, Younis SA (2021) Proof of concept for CUK family metal-organic frameworks as environmentally-friendly adsorbents for benzene vapor. Environ Pollut 285:117491. https://doi.org/10.1016/j.envpol.2021.117491
72. Osuchowski Ł, Szczęśniak B, Choma J, Jaroniec M (2019) High benzene adsorption capacity of micro-mesoporous carbon spheres prepared from XAD-4 resin beads with pores protected effectively by silica. J Mater Sci 54(22):13892–13900. https://doi.org/10.1007/s10853-019-03869-y
73. Hassan AA, Sorial GA (2010) Removal of benzene under acidic conditions in a controlled trickle bed air biofilter. J Hazard Mater 184(1–3):345–349. https://doi.org/10.1016/j.jhazmat.2010.08.042